BEPU ROBUSTNESS ANALYSIS VIA PERTURBED-LAW BASED SENSITIVITY INDICES

Bertrand Iooss, V Vergès, V Larget

BEPU ROBUSTNESS ANALYSIS VIA PERTURBED-LAW BASED SENSITIVITY INDICES

B. Iooss[1], V. Vergès[1] and V. Larget[2]
[1] EDF R&D, 6 Quai Watier, 78401, Chatou, France
[2] EDF DT, 19 rue Pierre Bourdeix, 69007 Lyon, France

bertrand.iooss@edf.fr, vanessa.verges@edf.fr, vincent.larget@edf.fr

ABSTRACT

One of the most critical hypothesis in BEPU studies is the choice of the probability distributions of uncertain input variables which are propagated through a numerical model. Depending on the method used for this choice, the probability density functions (pdf) for these variables are established with various levels of confidence, not always well known. Hence, bringing stringent justifications to the BEPU approach requires quantifying the impact of this second-level uncertainty (i.e. the uncertainty on the input variable pdf). To solve this problem, this paper deepens the robustness analysis based on the "Perturbed-Law based sensitivity Indices" (PLI). The PLI quantifies the impact of a perturbation of an input pdf on the quantity of interest (as a quantile of a model output or a safety margin) in the BEPU study. The mathematical formalism of the PLI is firstly applied to two particular quantities of interest: the quantile and the superquantile (which is the mean of the pdf tail exceeding the quantile). For both quantities, the PLI can be easily computed using a unique Monte-Carlo sample (ensemble of code runs) containing model inputs and output. Then, numerical tests are developed in order to define validity criteria of a PLI-based robustness analysis. The method is finally illustrated to the study of the thermal-hydraulic responses of a test facility during a cold leg Intermediate Break Loss Of Coolant Accident (IBLOCA) modelled using the calculation code CATHARE.

1. INTRODUCTION

One of the most critical hypothesis in classical BEPU and uncertainty quantification studies is the choice of the probability distributions of uncertain input variables which are propagated through a numerical model. Depending on the method used for this choice, the probability density functions (pdf) for these variables are established with various levels of confidence, not always well known. Hence, bringing stringent justifications to the BEPU approach requires quantifying the impact of this second-level uncertainty (i.e. the uncertainty on the input variable pdf) on the specific quantity of interest (QoI) related to the BEPU study.

To address such issues, the new branch of robustness analysis in uncertainty quantification has emerged during the recent years in the field of sensitivity analysis of model outputs [4]. It consists

of evaluating the impact of the choice of the inputs' distributions and, more precisely, by analyzing the QoI variations with respect to this choice. One particularly interesting solution has been proposed in the context of reliability-oriented sensitivity analysis by [11] with the Perturbed-Law based sensitivity Indices (PLI). This measure presents the important advantage to be not limited by the number of model inputs that can be considered. Another advantage of the PLI is that it explicitly focuses on a particular QoI, that has to be specified by the user. The QoI of most BEPU studies is a high-order (e.g. 95%) quantile of the model output variable [15, 13, 9]. However, in simulation-based risk analysis, several works [8, 10] have shown the interest of also considering the superquantile (i.e. the mean of the pdf tail exceeding the quantile) as a QoI. This risk measure gives interesting information about what is happening in the distribution-tail above the quantile. Its estimation also presents more regularities than those of the quantile estimation.

In this paper, the PLI-quantile concept [19, 20, 1] is extended to the PLI-superquantile one. Via intensive simulation studies, our work also addresses a fundamental question that arises in practice: which level of perturbations can be applied on an input pdf so that the method remains valid? The following section develops the mathematical formalism of the PLI applied to the quantile and superquantile. It shows that, for both the QoI, the PLI can be easily computed using a unique Monte-Carlo sample (ensemble of code runs) containing model inputs and output. Section 3 describes the numerical tests that allow to define validity criteria of a PLI-based robustness analysis. Section 4 illustrates the PLI approach to assess the robustness of a thermal-hydraulic simulation study (cold leg Intermediate Break Loss Of Coolant Accident) that uses the calculation code CATHARE. A conclusion section ends this paper.

2. PRINCIPLES OF PLI-QUANTILES AND PLI-SUPERQUANTILES

2.1 Introduction to PLI

Given the random vector $\mathbf{X} = (X_1, \ldots, X_d) \in \mathscr{X} \subseteq \mathbb{R}^d$ of d independent uncertain input variables of pdf $f(\mathbf{x}) = f_1(x_1) \times \ldots \times f_d(x_d)$, $G(\cdot)$ a numerical model and $Y = G(\mathbf{X}) \in \mathbb{R}$ the model output, the QoI is a statistical quantity derived from Y. For instance, it can be the mean, the variance, a quantile or a threshold exceedance probability of the model output.

A PLI aims to measure the impact of the modification of an input density on a QoI [11]. In order to compute the i-th PLI, we change the density f_i of X_i into a density $f_{i\delta}$, where $\delta \in \mathbb{R}$ represents the level of the perturbation. The PLI is then simply defined as the relative change in the QoI generated by the perturbation:

$$S_{i\delta} = \frac{\mathrm{QoI}_{i\delta} - \mathrm{QoI}}{\mathrm{QoI}} \,. \tag{1}$$

This definition slightly differs from the one proposed in previous studies [11, 20]. Indeed, after several applications of the PLI, it has been found more convenient to compute directly the relative variation of the quantile when submitted to a density perturbation [9]. The interpretation of PLI is then straightforward.

2.2 Quantiles and superquantiles

The quantile of order α of Y is

$$q^\alpha = q^\alpha(Y) = \inf\{t \in \mathbb{R}, F_Y(t) \geq \alpha\} \,, \tag{2}$$

where F_Y is the cumulative distribution function of the random variable Y. In BEPU studies, a high-order (e.g. 95%) quantile value is most often preferred to a failure probability computation, as it can easily be related to safety margin concepts [15].

However, the quantile does not give any information about what is happening in the distribution-tail above the quantile. Another quantity, called superquantile, giving more information about the distribution-tail has therefore been introduced [16]. A superquantile of order α is defined by

$$Q^\alpha = Q^\alpha(Y) = \mathbb{E}\left(\frac{G(\mathbf{X})\mathbb{1}_{G(\mathbf{X})\geq q^\alpha}}{1-\alpha}\right) \,, \tag{3}$$

where $\mathbb{E}(\cdot)$ denotes the expectation operator and $\mathbb{1}_A$ is the indicator function of the set A. If F_Y is continuous, we have the equivalence with the following definition [17]:

$$Q^\alpha = \mathbb{E}(G(\mathbf{X})|G(\mathbf{X}) \geq q^\alpha) \,. \tag{4}$$

Also known under the name of expected-shortfall and conditional-value-at-risk in finance, the superquantile has been proven to be a coherent risk measure (which is not the case for the quantile) [16, 8]. Moreover, its empirical estimator often presents more regularities than those of the quantile empirical estimator.

2.3 Estimation formulas

In a lot of applications, for instance in nuclear safety studies (see, e.g., [7]), the computer models are costly in terms of CPU time and memory. Only a limited number N of code runs is then available for the estimation of all the PLIs. The sample $\mathscr{X}_N = \{\mathbf{x}^{(n)} = (x_1^{(n)}, ..., x_d^{(n)})\}_{1\leq n\leq N}$ of N independent realizations of $\mathbf{X}$ (which follow the pdf f) is propagated through the model G to produce the sample $\mathscr{Y}_N = \{y_n\}_{1\leq n\leq N}$ of N model outputs. The most standard estimation of a quantile is based on the empirical quantile estimator denoted $\widehat{q}_N^\alpha = \inf\{t \in \mathbb{R}, \widehat{F}_Y^N(t) \leq \alpha\}$ where $\widehat{F}_Y^N(t) = \dfrac{1}{N}\sum_{n=1}^{N} \mathbb{1}_{y_n\leq t}$ is the empirical estimator of the cumulative density function of Y. The Wilks formula or the bootstrap technique can then be used to add a second level of conservatism (due to the limited size of the sample [21]). In this work, the bootstrap technique will be used.

From (2), the perturbed quantile writes:

$$q_{i\delta}^\alpha = \inf\{t \in \mathbb{R}, F_{Y,i\delta}(t) \geq \alpha\} \,, \tag{5}$$

with $F_{Y,i\delta}$ the cumulative distribution function corresponding to the input variable X_i sampled from $f_{i\delta}$. In order to give an estimation of the perturbed quantile (denoted $\widehat{q}_{N,i\delta}^\alpha$) from the same sample

$\mathscr{X}_N$, we use the so-called reverse importance sampling mechanism [3] to compute $\widehat{F}^N_{Y,i\delta}$ [1]:

$$\widehat{F}^N_{Y,i\delta}(t) = \frac{\sum_{n=1}^{N} L_i^{(n)} \mathbb{1}_{(y_n \leq t)}}{\sum_{n=1}^{N} L_i^{(n)}} , \tag{6}$$

with $L_i^{(n)}$ the likelihood ratio $\dfrac{f_{i\delta}(x_i^{(n)})}{f_i(x_i^{(n)})}$. We obtain $\widehat{q}^{\alpha}_{N,i\delta} = \inf\{t \in \mathbb{R}, \widehat{F}^N_{Y,i\delta}(t) \leq \alpha\}$. The estimator $\widehat{S}_{N,i\delta}$ of the PLI-quantile consists in replacing QoI by $\widehat{q}^{\alpha}_N$ in Eq. (1). Its theoretical properties (asymptotic consistence and central limit theorem) have been given in [2].

From (3), the perturbed superquantile writes:

$$Q^{\alpha}_{i\delta} = \mathbb{E}_{i\delta}\left(\frac{G(\mathbf{X})\mathbb{1}_{G(\mathbf{X}) \geq q^{\alpha}_{i\delta}}}{1-\alpha} \right) , \tag{7}$$

where $\mathbb{E}_{i\delta}$ means that the expectation is taken under the perturbed distribution $(f_1, \ldots, f_{i\delta}, \ldots, f_d)$. We define a biased version (used in the engineering study of [10]) of the perturbed superquantile:

$$Q'^{\alpha}_{i\delta} = \mathbb{E}\left(\frac{G(\mathbf{X})\mathbb{1}_{G(\mathbf{X}) \geq q^{\alpha}_{i\delta}}}{1-\alpha} \right) . \tag{8}$$

This equation gives a biased estimator because the expectation is taken under the initial distribution instead of the perturbed distribution. Its interest is that its estimation is easier and more stable (because the available sample is more representative of the initial distribution than the perturbed distribution).

In order to give an estimation of these quantities from the sample $(\mathscr{X}_N, \mathscr{Y}_N)$, we use the same mechanism as before by using the discretized-integral formula

$$\widehat{Q}^{\alpha}_{N,i\delta} = \frac{1}{1-\alpha} \sum_{n=1}^{N} G(\mathbf{x}^{(n)}) \mathbb{1}_{G(\mathbf{x}^{(n)}) \geq \widehat{q}^{\alpha}_{N,i\delta}} L_i^{(n)} f(\mathbf{x}^{(n)}) . \tag{9}$$

The estimator $\widehat{S}_{N,i\delta}$ of the PLI-superquantile consists in replacing QoI by $\widehat{Q}^{\alpha}_N$ in Eq. (1). For the biased PLI-superquantile estimation, we simply write:

$$\widehat{Q}'^{\alpha}_{N,i\delta} = \frac{1}{1-\alpha} \sum_{n=1}^{N} G(\mathbf{x}^{(n)}) \mathbb{1}_{G(\mathbf{x}^{(n)}) \geq \widehat{q}^{\alpha}_{N,i\delta}} f(\mathbf{x}^{(n)}) . \tag{10}$$

In the following, the estimator $\widehat{S}_{N,i\delta}$ will be denoted $\widehat{S}_{i\delta}$.

2.4 Input density perturbation method

The density perturbation approach proposed in [11] (and used in [20, 6]) consists of replacing the density f_i of one input X_i by a perturbed one $f_{i\delta}$, where $\delta \in \mathbb{R}$ represents a shift of a moment (e.g.

the mean or the variance). Amongst all densities with shifted mean or variance of a δ value, $f_{i\delta}$ is defined as the one minimizing the Kullback-Leibler divergence from f_i. Figure 1 illustrates some perturbed pdf after a perturbation on the mean of initial pdf. Increasing the mean of a Gaussian pdf just consists in translating it by a constant shift (the perturbed pdf remains Gaussian). Increasing the mean of a uniform pdf turns to a non-uniform pdf (because we force its support to be fixed) which gives more weights to the large values.

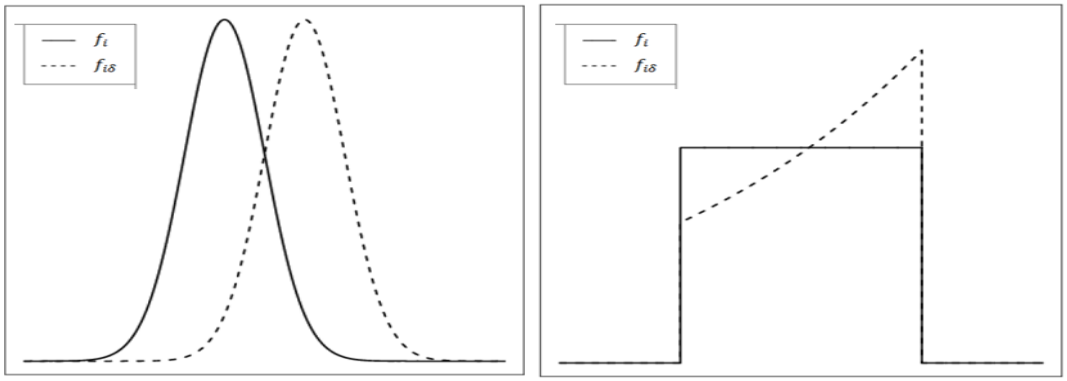

Figure 1: Examples of perturbed pdf for Gaussian (left) and uniform (right) initial pdf and a perturbation on the mean.

In the following, we focus on one type of perturbations used in most of the studies, that is the perturbation of the mean of the random variable. However, even in this simplest perturbation case, minimizing the Kullback-Leibler divergence can be difficult or even impossible for some particular distributions (such as the log-normal one) [11]. A simpler approach proposed in [14] starts by applying an iso-probabilistic operator (such as the Rosenblatt transform) to the initial input pdf, in order to transform all the input random variables into centered normalized Gaussian ones (denoted $\mathcal{N}(0,1)$). In case of independent inputs, it just corresponds to the inverse probability distribution transform. Then, the perturbations are applied on Gaussian pdf (as in Figure 1, left) and the solution is trivial as the perturbed pdf is $\mathcal{N}(\delta,1)$ where δ is the perturbation level. This method allows to make perturbations comparable when applied in this standard space [1, 14, 9].

In practice, one has to define the variation range of δ as it can be of interest to decrease and increase it. Looking at the PLI evolution as a function of δ will be also informative. To illustrate this, we compute the PLI-quantile at order $\alpha = 0.95$ on the linear model output $Y = 2X_1 + X_2 + X_3/2$ with $X_i \sim \mathcal{N}(0,1)$ for $i = 1,2,3$. The estimations are made by using a Monte Carlo sample $(\mathscr{X}_N, \mathscr{Y}_N)$ of size $N = 5000$, by applying a mean perturbation on the range $\delta \in [-1,1]$. Figure 2 shows the PLI curve for each input. In this linear model case, the PLI curves are linear because the output quantile increases linearly with the increase of each input mean. Moreover, the larger weight of X_1 in the model equation explains its larger impact than that of X_2 and X_3.

Thanks to the use of a Monte Carlo sample, applying a bootstrap technique allows to associate a confidence interval (CI) to each PLI estimate. In the rest of this paper, 95%-CI will be considered, most often computed with $R = 100$ bootstrap replicas (when simulations are too expensive $R = 50$ replicas are taken). Evaluating this estimation uncertainty is crucial in practice as the limited sample size can lead to erroneous result from a certain level of perturbation (e.g. when there

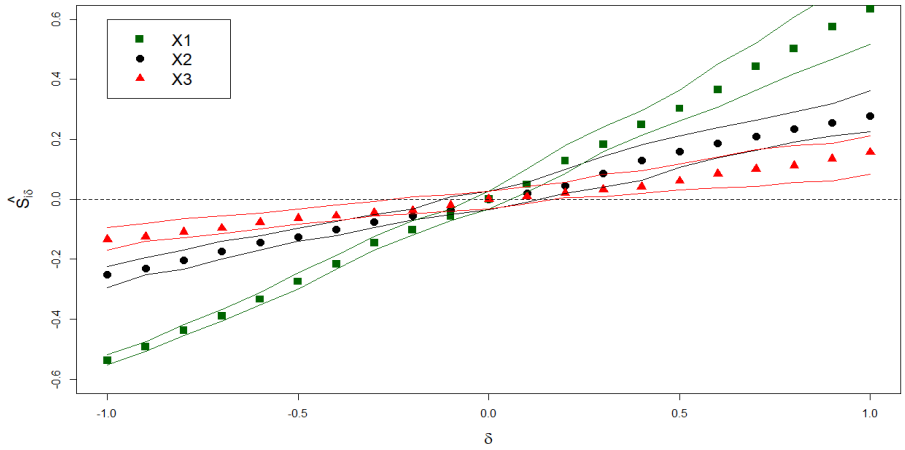

Figure 2: PLI-quantile ($\alpha = 0.95$) for the linear model. The points are the PLI at different discretized values of δ. The lines are the corresponding bootstrap 95%-confidence intervals.

are not enough sample values close to the perturbed quantile). Our PLI-CI is computed from the perturbed quantile CI, by bootstrap resampling of the Monte Carlo sample. Then, it fully integrates the uncertainty due to the limited size of the sample (this is why the CI does not collapse at $\delta = 0$).

3. NUMERICAL VALIDATION TESTS

In order to validate the PLI-based robustness analysis, we develop in this section several numerical tests on toy functions with a small number of inputs (three inputs $X_i \sim \mathcal{N}(0,1)$ for $i = 1,2,3$). Note that the method can be applied to large-dimensional models and non-Gaussian inputs as it will be shown in Section 4. The two toy models are the linear model shown in Section 2.4:

$$Y = 2X_1 + X_2 + X_3/2 \,, \tag{11}$$

and the Ishigami function:

$$Y = \sin(X_1) + 7\sin^2(X_2) + 0.1X_3^4 \sin(X_1) \,. \tag{12}$$

The PLI-quantile and PLI-superquantile estimation (which are based on the same principles) are studied by applying a mean perturbation on the range $\delta \in [-3,3]$.

In Figure 3, the PLI-quantile (first and second lines) and PLI-superquantile (third and fourth lines) are computed on the linear model and with $\alpha = 0.95$, by using a Monte Carlo sample $(\mathscr{X}_N, \mathscr{Y}_N)$ of size $N = 1000$ (first and third lines) and $N = 10000$ (second and fourth lines). The left column consists in comparing the PLI estimates in black (formulas of Section 2.3) with the reference results based on resimulations in red (i.e. results that would be obtained without the reverse sampling procedure but by resampling the input following the perturbed pdf). We can observe that the PLI (and the PLI-CI) are valid in the central zone of the plots (centered on the value $\delta = 0$) and turn to be invalid at large δ values (when red CI are not inside black CI). Moreover, increasing the sample size extends the PLI-CI validity domain with respect to the δ variation range. Indeed, as

the sample size is finite, at a certain level of perturbation, there is not enough sample values to correctly compute the perturbed quantile and its CI.

From these findings, two heuristics are proposed to provide warnings to users when δ is too large:

1. The number of values in $\mathscr{X}_N$, smaller or larger of the δ-perturbed mean of an input variable, has to be sufficient. A value of $N_x = 30$ has been chosen (from several numerical tests) as the smallest size, but can be changed. This criterion is easily computed from $\mathscr{X}_N$ and each δ-value. It is represented by the green vertical lines on each plot.

2. The number of values in $\mathscr{Y}_N$, smaller or larger of the δ-perturbed quantile of the model output, has to be sufficient. A value of $N_y = 5$ (resp. $N_y = 10$) has been chosen (from several numerical tests) as the smallest size for the PLI-quantile (resp. PLI-superquantile), but can be changed. It is represented by the blue vertical line on each plot.

In Figure 3 (left column), these two criteria are visualized and show their relevance to warn the user that the PLI values (and their CI) no longer make sense beyond these limits (e.g. because PLI-CI do not contain the PLI reference values). Of course, the green and blue vertical lines are not visible in the plots when they are outside of the δ variation range.

The right column of Figure 3 visualizes the uncertainty on the PLI-CI by showing the 95%-CI of the PLI-CI lower bound (in orange) and the 95%-CI of the PLI-CI upper bound (in red). It aims to visualize the stability of the PLI-CI, knowing that looking at the value of the PLI should not be done without looking at its associated CI. We verify that, beyond the limits given by the green and blue vertical lines, the CIs of the lower and upper bounds of the PLI-CI explode.

The validity results for the Ishigami function are given in Figure 4, by using a Monte Carlo sample $(\mathscr{X}_N, \mathscr{Y}_N)$ of size $N = 1000$, for the PLI-quantile (first and third lines) and PLI-superquantile (second and fourth lines) with $\alpha = 0.75$, for X_1 (first and second lines) and X_2 (third and fourth lines). The results show similar behavior than the linear model ones and confirm the relevance of the two heuristic validation criteria.

4. APPLICATION on IB-LOCA

As a nuclear facility operator, EDF has to perform safety analysis on his pressurized water nuclear reactors, those studies include the "Loss of Coolant Accident" (LOCA) resulting in a break on the primary loop of the reactor. This scenario is simulated using system thermal-hydraulic computer codes, which include tens of physical parameters such as condensation or heat transfer coefficients [12, 18]. Yet, the values of the model parameters are known with a limited precision as they are evaluated through tests performed on small-scale experimental facilities. Some other variables are only observed during periodic inspections, such as the characteristics of hydraulics systems.

The case of application is a 4-loop reactor from the French fleet[1]. The transient studied is an IB-LOCA, the break considered is a 13-inches break located on the cold leg. The reactor is supposed

[1]The input data considered for this case, and thus the PCT reached do not correspond to actual industrial values

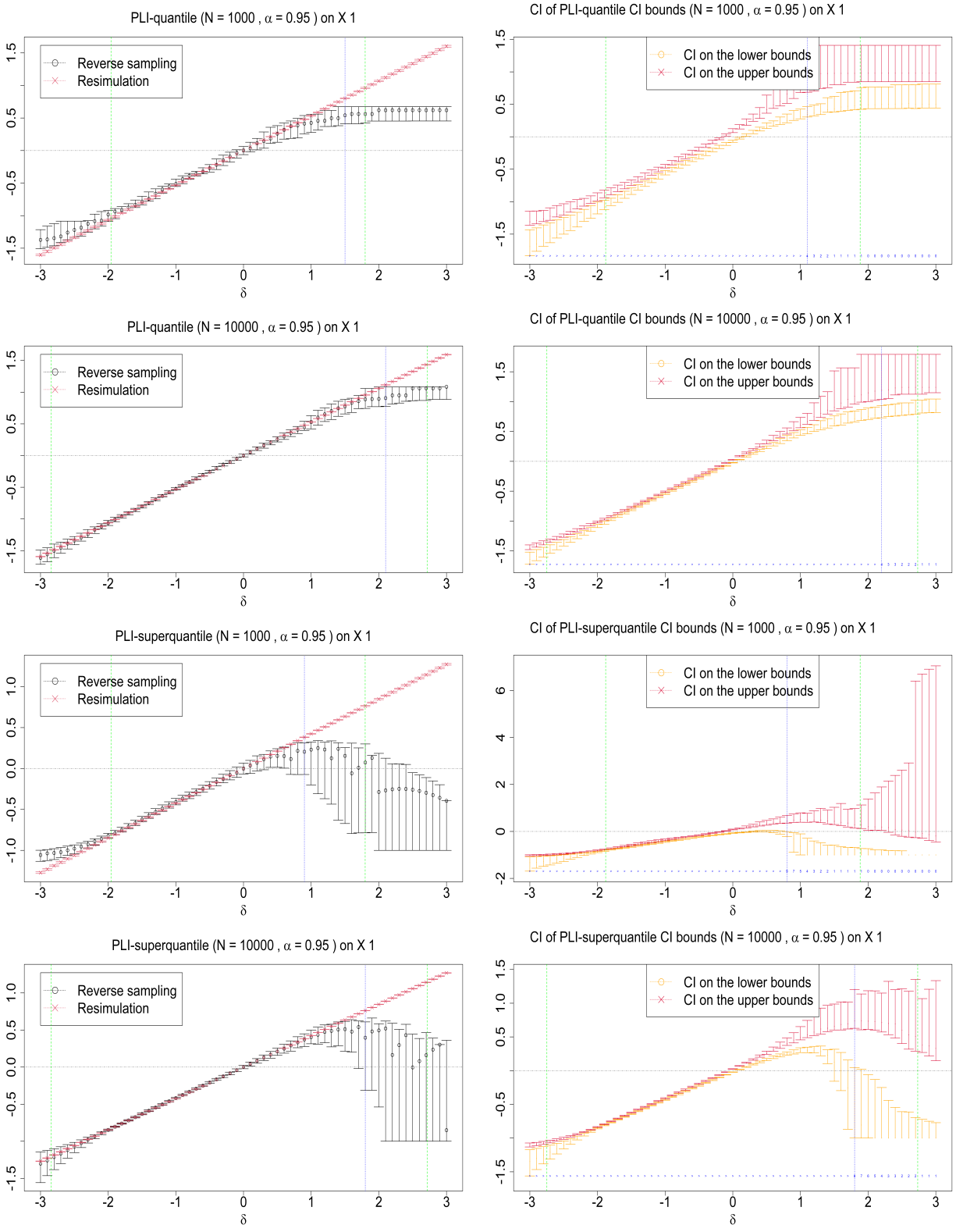

Figure 3: PLI validation results applied on X_1 of the linear model.

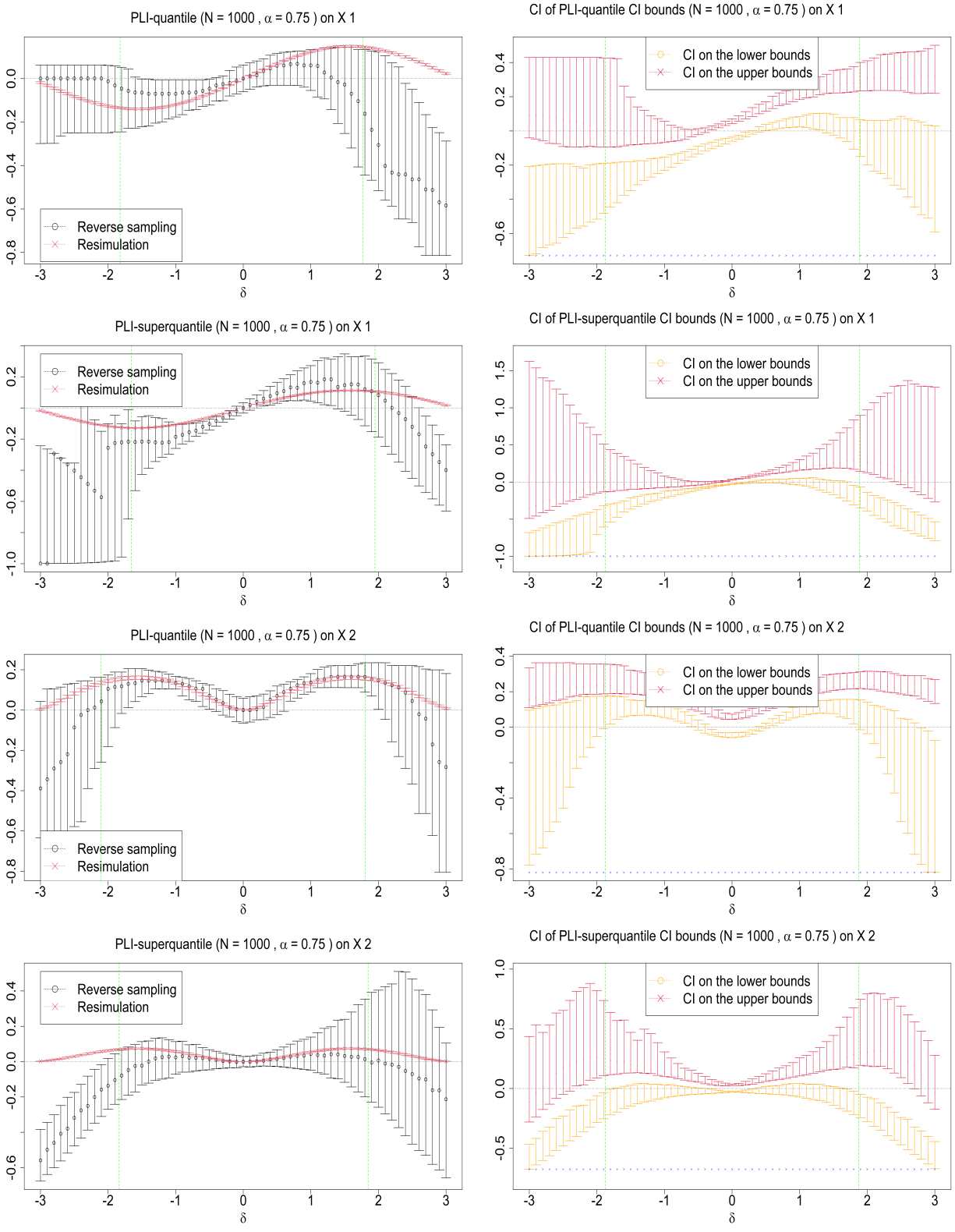

Figure 4: PLI validation results applied on X_1 and X_2 of the Ishigami function.

to be at nominal power at the opening of the break. The main common assumptions for LOCA safety analysis are considered. The availability of the systems is assumed to be restricted to the minimum safety systems (ECCS, EFWS, ...), other systems are considered to be unavailable. The most limiting additional single failure is postulated.

The LOCA transients are simulated using the CATHARE code developed by the CEA, EDF, Framatome and IRSN. In our simulation scenario, $d \approx 100$ random inputs are considered and the output variable of interest is the second peak cladding temperature (PCT). For each input, depending on its nature and the information available on it, a pdf type (e.g. uniform, truncated Gaussian, truncated lognormal, triangular) is chosen, in concordance with its parameters. A Monte Carlo sample of $N = 2000$ input and output values have then be generated.

The QoI for this study is 95%-quantile and 75%-superquantile of the PCT, which is estimated from the Monte Carlo sample at $q^{0.95} = 737°\text{C}$ and $Q^{0.75} = 673°\text{C}$. Our PLI approach consists in transforming each input pdf in a $\mathcal{N}(0,1)$ one, then perturbing the mean of each input with $\delta \in [-1.64, 1.64]$. This range corresponds to the 5%-quantile and 95%-quantile of a $\mathcal{N}(0,1)$ variable. The Figure 5 illustrates several perturbed empirical pdf from the Monte Carlo sample for four different variables.

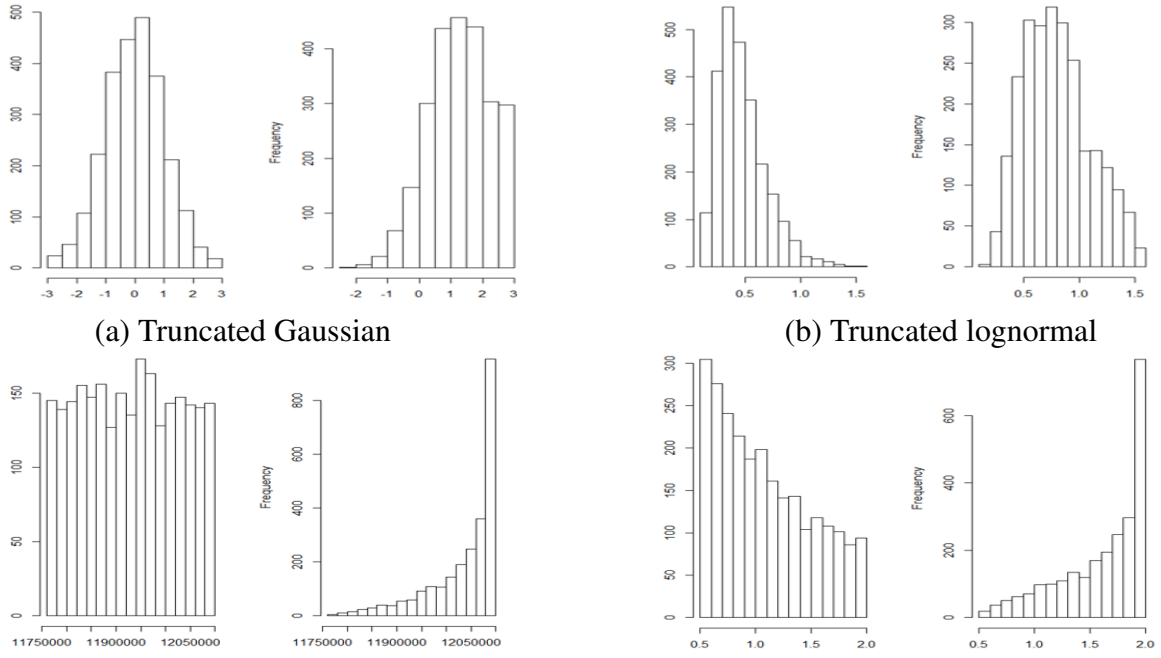

(a) Truncated Gaussian (b) Truncated lognormal

(c) Uniform (b) Triangular

Figure 5: Examples of perturbed pdf for four inputs with different pdf of the IB-LOCA case. Each case (a, b, c, d) shows the initial pdf (left) and the perturbed pdf by taking $\delta = 1.28$ (right)

On this high dimensional industrial application case (100 inputs), PLI can be easily computed but visualizing a large number of PLI curves remain a challenge. Therefore, only 8 inputs with strong influence (described in Table 1) are shown in Figure 6 through their PLI-quantile and PLI-superquantile curves. Validity criteria do not appear on the plots because the size of the Monte

Variable	Variable description	Distribution
X52	Minimum Stable Film Temperature	Uniform
X64	HTC wall-steam exchange in C7 zone	Log-Normal
X76	HTC primary-secondary - Natural liquid convection in SG	Log-Uniform
X78	Wall-steam friction coefficient (CV) in HA	Log-Uniform
X110	Interfacial friction in the downcomer	Log-Normal
X111	Interfacial friction in the core during blowdown phase	Log-Normal
X113	Bubble-rise velocity in the upper plenum	Log-Normal
X116	Bubble-rise velocity in the upper head	Log-Normal

Table 1: Definition of the 8 parameters considered for the PLI calculations. All the log-normal distributions are truncated.

Carlo sample is sufficient with respect to the perturbation values that have been considered.

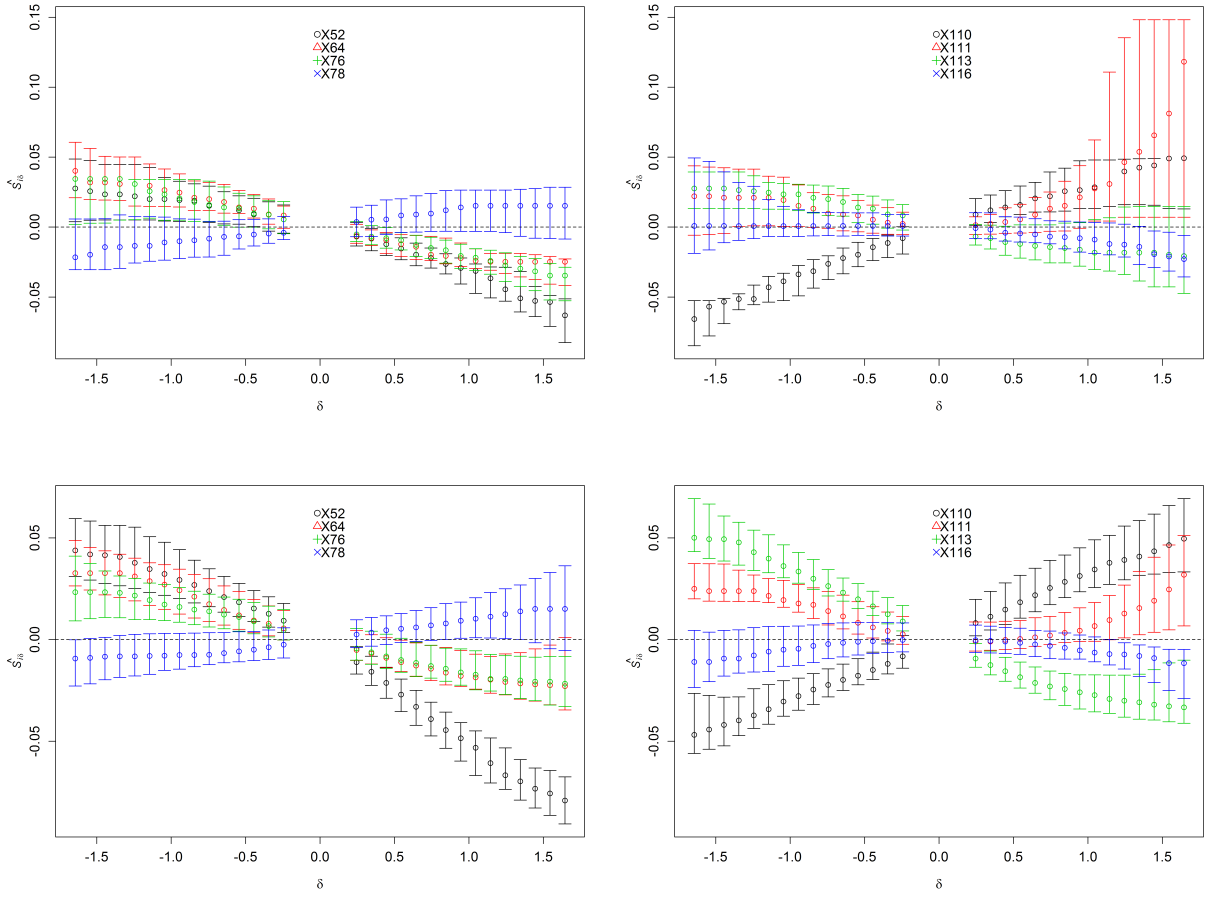

Figure 6: PLI-0.95-quantile (upper panels) and PLI-0.75-superquantile (lower panels) of the IB-LOCA case.

By comparing the results of PLI-quantile and PLI-superquantile, we observe that both PLI give the same trends. However, differences can be noted on the most influential parameters, depending on the level of perturbation δ reached. Furthermore, PLI clearly determine the penalizing variation direction of each input: the QoI (0.95-quantile and 0.75-superquantile of the PCT) increase with an increase of the friction coefficients (X78, X110 and X111) and a decrease of the stable film temperature (X52), the exchange coefficients (X64 and X76) and the bubble-rise velocity X113. Decreasing X111 also leads to an increase of the QoI which allows to emphasize the non-monotonic behavior of the PCT with respect to the interfacial friction in the core during blowdown phase. Such information is precious for discussing BEPU results.

On Figure 6, one important observation is the behavior of the confidence interval when δ is high. For some variables, for example X111 on the PLI-quantile calculation, a saturation of the CI occur for high values of δ. This is due to the limited number of value of the output exceeding the quantile. That behavior is not observed in the PLI-superquantile calculation because of the inherent regularity of the superquantile, and the fact that the level of superquantile considered is low enough. This phenomenon seems to be fostered by the combination of PLI-quantile at high quantile level and strong perturbation. Thus, for further industrial applications, in order to have the most accurate estimation of the PLI, the use of PLI-superquantile associated to limited value of δ (typically $\delta \leq 1$) should be considered. This recommendation has already been considered in the industrial methodology presented in [10].

5. CONCLUSION

In the context of uncertainty quantification studies and in particular when applying BEPU methodologies, hypotheses have to be made in order to define the input distributions which are not always easy to justify. This work has focused on the PLI approach which allows to challenge the hypotheses made on the uncertain input pdf. The main goal of PLI is to quantify the robustness of a BEPU QoI with respect to uncertainty on the pdf of the model inputs. However, PLI is also a sensitivity measure which quantifies the influence of each input on the QoI. In this paper, PLI has allowed to quantify the impact of each input mean on quantiles and superquantiles. Finally, an important contribution of this work rely in the introduction of new criteria for studying the validity of the PLI analysis.

This approach has been applied to an IB-LOCA scenario simulated with the CATHARE code. In addition to the rich information that is provided on the inputs' influence and on the QoI robustness, it has enlightened the two important advantages of the PLI approach: it only needs a simple Monte Carlo sample and it is not limited in terms of number of model inputs.

To develop more deeply the PLI, further works have to focus on more general perturbation type [2], on developing multivariate PLI, on considering the dependent inputs case and on using more efficient sampling technique than Monte Carlo scheme (as the importance sampling one [19]).

6. ACKNOWLEDGMENTS

We thank Jérôme Stenger for his help on theoretical aspects of PLI-superquantiles. Numerical computations of the PLI have been realized using the sensitivity package [5] of the R software.

7. REFERENCES

[1] T. Delage, R. Sueur, and B. Iooss. Robustness analysis of epistemic uncertainties propagation studies in LOCA assessment thermal-hydraulic model. In *Proceedings of ANS Best Estimate Plus Uncertainty International Conference (BEPU 2018)*, Lucca, Italy, may 2018.

[2] C. Gauchy, J. Stenger, R. Sueur, and B. Iooss. An information geometry approach for robustness analysis in uncertainty quantification of computer codes. *Preprint*, 2019, URL https://hal.archives-ouvertes.fr/hal-02425477.

[3] T.C. Hesterberg. Estimates and confidence intervals for importance sampling sensitivity analysis. *Mathl. Comput. Modelling*, 23:79–85, 1996.

[4] B. Iooss. Sensitivity analysis of model outputs: methods and issues for BEPU methodology. In *Proceedings of ANS Best Estimate Plus Uncertainty International Conference (BEPU 2018)*, Lucca, Italy, may 2018.

[5] B. Iooss, S. Da Veiga, A. Janon, and G. Pujol. *sensitivity: Global Sensitivity Analysis of Model Outputs*, 2020. R package version 1.19.0.

[6] B. Iooss and L. Le Gratiet. Uncertainty and sensitivity analysis of functional risk curves based on Gaussian processes. *Reliability Engineering and System Safety*, 187:58–66, 2019.

[7] B. Iooss and A. Marrel. Advanced methodology for uncertainty propagation in computer experiments with large number of inputs. *Nuclear Technology*, 205:1588–1606, 2019.

[8] T. Labopin-Richard, F. Gamboa, A. Garivier, and B. Iooss. Bregman superquantiles. Estimation methods and applications. *Dependence Modeling*, pages 76–108, 2016.

[9] V. Larget. How to bring conservatism to a BEPU analysis. In *NURETH-18*, Portland, USA, August 2019.

[10] V. Larget and M. Gautier. Increasing conservatism in BEPU IB LOCA safety studies using complementary and industrially cost effective statistical tools. In *Submitted to the ANS Best Estimate Plus Uncertainty International Conference (BEPU 2020)*, Giardini Naxos, Italy, october 2020.

[11] P. Lemaître, E. Sergienko, A. Arnaud, N. Bousquet, F. Gamboa, and B. Iooss. Density modification based reliability sensitivity analysis. *Journal of Statistical Computation and Simulation*, 85:1200–1223, 2015.

[12] P. Mazgaj, J-L. Vacher, and S. Carnevali. Comparison of CATHARE results with the experimental results of cold leg intermediate break LOCA obtained during ROSA-2/LSTF test 7. *The European Journal of Physics - Nuclear Sciences & Technology (EPJ-N)*, 2(1), 2016.

[13] V. Mousseau and B.J. Williams. Uncertainty quantification in a regulatory environment. In R. Ghanem, D. Higdon, and H. Owhadi, editors, *Springer Handbook on Uncertainty Quantification*, pages 1613–1648. Springer, 2017.

[14] G. Perrin and G. Defaux. Efficient estimation of reliability-oriented sensitivity indices. *Journal of Scientific Computing*, 80(3), 2019.

[15] A. Prosek and B. Mavko. The state-of-the-art theory and applications of best-estimate plus uncertainty methods. *Nuclear Technology*, 158:69–79, 2007.

[16] R.T. Rockafellar. Coherent approaches to risk in optimization under uncertainty. *Tutorials in Operations Research INFORMS 2007*, pages 38–61, 2007.

[17] R.T. Rockafellar and S. Uryasev. Conditional value-at-risk for general loss distributions. *Journal of Banking & Finance*, 26:1443–1471, 2002.

[18] F. Sanchez-Saez, A.I. Sànchez, J.F. Villanueva, S. Carlos, and S. Martorell. Uncertainty analysis of large break loss of coolant accident in a pressurized water reactor using non-parametric methods. *Reliability Engineering and System Safety*, 174:19–28, 2018.

[19] R. Sueur, N. Bousquet, B. Iooss, and J. Bect. Perturbed-law based sensitivity indices for sensitivity analysis in structural reliability. In *Proceedings of the 8th International Conference on Sensitivity Analysis of Model Output (SAMO 2016)*, Le Tampon, Réunion Island, France, December 2016.

[20] R. Sueur, B. Iooss, and T. Delage. Sensitivity analysis using perturbed-law based indices for quantiles and application to an industrial case. In *Proceedings of the 10th International Conference on Mathematical Methods in Reliability (MMR 2017)*, Grenoble, France, 2017.

[21] E. Zio and F. Di Maio. Bootstrap and order statistics for quantifying thermal-hydraulic code uncertainties in the estimation of safety margins. *Science and Technology of Nuclear Installations*, 2008(Article ID 340164, 9 pages, DOI:10.1155/2008/340164), 2008.